

Flux Synthesis, Crystal Structure, and Luminescence Properties of a New Europium Fluoride–Silicate: $K_5Eu_2FSi_4O_{13}$

Pei-Yun Chiang,[†] Tsai-Wei Lin,[†] Jian-Hung Dai,[†] Bor-Chen Chang,^{*,†} and Kwang-Hwa Lii^{*,†,‡}

Department of Chemistry, National Central University, Chungli, Taiwan, R.O.C., and
Institute of Chemistry, Academia Sinica, Taipei, Taiwan, R.O.C.

Received January 9, 2007

The crystal structure and luminescence properties of flux-grown crystals of a new europium(III) fluoride–silicate, $K_5Eu_2FSi_4O_{13}$, are reported. The structure consists of octahedral dimers of the composition $[Eu_2O_{10}F]$, which are linked by unbranched tetrasilicate chains to form a 3-D framework with 5- and 6-ring channels parallel to the *b* axis where the K^+ cations are located. The sharp peaks in the room-temperature emission spectrum are assigned. The number of lines in the region for the $^5D_0 \rightarrow ^7F_0$ transition and the relative intensities of the $^5D_0 \rightarrow ^7F_1$ and $^5D_0 \rightarrow ^7F_2$ transitions confirm the presence of two local Eu^{3+} environments and strongly distorted Eu^{3+} –ligand surroundings. The room-temperature fluorescence decay curves are well fit by a single-exponential function yielding a lifetime value of about 2.0 ms. Crystal data: monoclinic, space group $P2_1/m$, $a = 7.1850(2)$ Å, $b = 5.7981(2)$ Å, $c = 18.1675(6)$ Å, $\beta = 92.248(2)^\circ$, and $Z = 2$.

Introduction

A large number of silicates containing transition metals,^{1–8} main-group elements,^{9–13} lanthanide elements,^{14–24} and uranium^{25–31} have been reported. They have shown a rich structural chemistry and interesting physical and chemical

properties. In contrast to zeolites, which are built of $[SiO_4]^{4-}$ and $[AlO_4]^{5-}$ tetrahedra, these silicate frameworks contain metals in different coordination geometries. Recently Rocha and co-workers synthesized a good number of lanthanide silicates with the main aim of combining, in a given silicate, microporosity and optical activity.^{14–17} Lanthanide-containing compounds are interesting luminescent materials because

* To whom correspondence should be addressed. E-mail: liikh@cc.ncu.edu.tw (K.-H.L.), bcchang@cc.ncu.edu.tw (B.-C.C.).

[†] National Central University.

[‡] Academia Sinica.

- (1) Rocha, J.; Anderson, M. W. *Eur. J. Inorg. Chem.* **2000**, 801.
- (2) Wang, X.; Liu, L.; Jacobson, A. J. *Angew. Chem., Int. Ed.* **2001**, *40*, 2174.
- (3) Wang, X.; Liu, L.; Jacobson, A. J. *J. Am. Chem. Soc.* **2002**, *124*, 7812.
- (4) Brandão, P.; Valente, A.; Philippou, A.; Ferreira, A.; Anderson, M. W.; Rocha, J. *Eur. J. Inorg. Chem.* **2003**, 1175.
- (5) Nyman, M.; Bonhomme, F.; Teter, D. M.; Maxwell, R. S.; Bu, B. X.; Wang, L. M.; Ewing, R. C.; Nenoff, T. M. *Chem. Mater.* **2000**, *12*, 3449.
- (6) Nyman, M.; Bonhomme, F.; Maxwell, R. S.; Nenoff, T. M. *Chem. Mater.* **2001**, *13*, 4603.
- (7) Francis, R. J.; Jacobson, A. J. *Angew. Chem., Int. Ed.* **2001**, *40*, 2879.
- (8) Kao, H.-M.; Lii, K.-H. *Inorg. Chem.* **2002**, *41*, 5644.
- (9) Ferreira, A.; Lin, Z.; Rocha, J.; Morais, C. M.; Lopes, M.; Fernandez, C. *Inorg. Chem.* **2001**, *40*, 3330.
- (10) Ferreira, A.; Lin, Z.; Soares, M. R.; Rocha, J. *Inorg. Chim. Acta* **2003**, *356*, 19.
- (11) Hung, L.-I.; Wang, S.-L.; Szu, S.-P.; Hsieh, C.-Y.; Kao, H.-M.; Lii, K.-H. *Chem. Mater.* **2004**, *16*, 1660.
- (12) Hung, L.-I.; Wang, S.-L.; Chen, C.-Y.; Chang, B.-C.; Lii, K.-H. *Inorg. Chem.* **2005**, *44*, 2992.
- (13) Liao, C.-H.; Chang, P.-C.; Kao, H.-M.; Lii, K.-H. *Inorg. Chem.* **2005**, *44*, 9335.
- (14) Rocha, J.; Ferreira, P.; Carlos, L. D.; Ferreira, A. *Angew. Chem., Int. Ed.* **2000**, *39*, 3276.

- (15) Ananias, D.; Ferreira, A.; Rocha, J.; Ferreira, P.; Rainho, J. P.; Morais, C.; Carlos, L. D. *J. Am. Chem. Soc.* **2001**, *123*, 5735.
- (16) Ferreira, A.; Ananias, D.; Carlos, L. D.; Morais, C. M.; Rocha, J. *J. Am. Chem. Soc.* **2003**, *125*, 14573.
- (17) Ananias, D.; Kostova, M.; Almeida Paz, F. A.; Ferreira, A.; Carlos, L. D.; Klinowski, J.; Rocha, J. *J. Am. Chem. Soc.* **2004**, *126*, 10410.
- (18) Jeong, H.-K.; Chandrasekaran, A.; Tsapatsis, M. *Chem. Commun.* **2002**, 2398.
- (19) Haile, S. M.; Wuensch, B. J. *Acta Crystallogr.* **2000**, *B56*, 335.
- (20) Haile, S. M.; Wuensch, B. J. *Acta Crystallogr.* **2000**, *B56*, 349.
- (21) Kolitsch, U.; Tillmanns, E. *Mineral. Mag.* **2004**, *68*, 677.
- (22) Huang, M.-Y.; Chen, Y.-H.; Chang, B.-C.; Lii, K.-H. *Chem. Mater.* **2005**, *17*, 5743.
- (23) Wang, G.; Li, J.; Yu, J.; Chen, P.; Pan, Q.; Song, H.; Xu, R. *Chem. Mater.* **2006**, *18*, 5637.
- (24) Ananias, D.; Almeida Paz, F. A.; Carlos, L. D.; Geraldes, C. F. G. C.; Rocha, J. *Angew. Chem., Int. Ed.* **2006**, *45*, 7938.
- (25) Wang, X.; Huang, J.; Jacobson, A. J. *J. Am. Chem. Soc.* **2002**, *124*, 15190.
- (26) Huang, J.; Wang, X.; Jacobson, A. J. *J. Mater. Chem.* **2003**, *13*, 191.
- (27) Burns, P. C.; Olson, R. A.; Finch, R. J.; Hanchar, J. M.; Thibault, Y. *J. Nucl. Mater.* **2000**, *278*, 290.
- (28) Burns, P. C. *Can. Mineral.* **2005**, *43*, 1839.
- (29) Chen, C.-S.; Kao, H.-M.; Lii, K.-H. *Inorg. Chem.* **2005**, *44*, 935.
- (30) Chen, C.-S.; Chiang, R. K.; Kao, H.-M.; Lii, K.-H. *Inorg. Chem.* **2005**, *44*, 3914.
- (31) Chen, C.-S.; Lee, S.-F.; Lii, K.-H. *J. Am. Chem. Soc.* **2005**, *127*, 12208.

they emit over the entire spectral range as near-infrared (Nd^{3+} , Er^{3+}), red (Eu^{3+} , Pr^{3+} , Sm^{3+}), green (Er^{3+} , Tb^{3+}), and blue (Tm^{3+} , Ce^{3+}). These lanthanide silicates were synthesized with alkali metal cations in a Teflon-lined autoclave under mild hydrothermal conditions at 180–240 °C. Wang et al. reported a new luminescent microporous terbium silicate containing 9-ring channels.²³ The same structure for a wider range of lanthanide ions and the very unusual photoluminescence properties of this system were also reported by Ananias et al.²⁴ Crystals of several lanthanide silicates were grown under high-temperature and high-pressure hydrothermal conditions by Haile et al. to search for fast alkali metal ion conductors.^{19,20} We previously reported the high-temperature/high-pressure hydrothermal synthesis, single-crystal X-ray structure, and luminescence properties of a new europium silicate, $\text{Cs}_3\text{EuSi}_6\text{O}_{15}$.²² This is the second example of a 3-D silicate framework with $\text{Si}/\text{O} = 2/5$, which contains only tertiary $[\text{SiO}_4]$ tetrahedra. Lanthanide silicates can also be synthesized by using flux-growth techniques. Kolitsch and Tillmanns reported a new microporous silicate, $\text{Cs}_3\text{ScSi}_8\text{O}_{19}$,²¹ which was synthesized from a CsF – MoO_3 flux. In an attempt to extend our studies to explore whether we can synthesize new lanthanide silicates by using the flux-growth method, we obtained a new europium(III) fluoride tetrasilicate. The present paper presents the flux synthesis, single-crystal X-ray structure, and luminescence properties of $\text{K}_5\text{Eu}_2\text{FSi}_4\text{O}_{13}$ (denoted as **1**).

Experimental Section

Synthesis. Compound **1** was synthesized from a KF – MoO_3 flux. A mixture of 0.666 g of KF , 0.333 g of MoO_3 , 0.0988 g of Eu_2O_3 , and 0.1012 g of SiO_2 ($\text{K}/\text{Eu}/\text{Si}$ mole ratio = 20.2/1/3) was placed in a 4 mL platinum crucible, heated to 900 °C, and isothermed for 10 h, followed by slow cooling to 750 °C at 2 °C/h and then furnace cooling to room temperature. The flux was dissolved with hot water, and the solid product was obtained by suction filtration. The reaction produced colorless tablet crystals of **1** as the only product, as indicated by powder X-ray diffraction (Supporting Information, Figure S1). Powder X-ray data were collected in the range of $5^\circ \leq 2\theta \leq 50^\circ$ on a Shimadzu XRD-6000 automated powder diffractometer using the θ – 2θ mode in a Bragg–Brentano geometry. Energy dispersive X-ray analysis of several crystals showed the presence of K, Eu, Si, F, and O. The yield of **1** was 86.2% based on Eu. A crystal was selected for indexing and intensity data collection.

Single-Crystal X-ray Diffraction. A suitable crystal of **1** with dimensions of $0.05 \times 0.05 \times 0.25 \text{ mm}^3$ was selected for indexing and intensity data collection on a Bruker CCD diffractometer. Intensity data were collected at room temperature in 1271 frames with ω scans (width 0.30° per frame). The program SADABS was used for absorption correction ($T_{\text{min,max}} = 0.575, 0.952$). The structure was solved by direct methods and difference-Fourier syntheses. To balance the charge, the atom bonded to two Eu atoms was assigned to F. We earlier refined the structure with an O atom at this bridging position. The atom exhibited a nonpositive definite atom displacement factor and a very small equivalent isotropic atom displacement factor. Bond-valence calculation indicated that all O atoms had valence sums close to 2 and the bridging F atom had a value of 0.91.³² The final cycles of least-squares refinement included atomic coordinates and anisotropic thermal parameters for all atoms.

Table 1. Crystallographic Data for $\text{K}_5\text{Eu}_2\text{FSi}_4\text{O}_{13}$

chemical formula	$\text{FK}_5\text{O}_{13}\text{Eu}_2\text{Si}_4$
$a/\text{\AA}$	7.1850(2)
$b/\text{\AA}$	5.7981(2)
$c/\text{\AA}$	18.1675(6)
β/deg	92.248(2)
$V/\text{\AA}^3$	756.26(7)
Z	2
fw	838.78
space group	$P2_1/m$ (No. 11)
$T/^\circ\text{C}$	23
$\lambda(\text{Mo K}\alpha)/\text{\AA}$	0.71073
$D_{\text{calc}}/\text{g}\cdot\text{cm}^{-3}$	3.683
$\mu(\text{Mo K}\alpha)/\text{cm}^{-1}$	99.9
R_1^a	0.0256
wR_2^b	0.0662

^a $R_1 = \sum ||F_o| - |F_c|| / \sum |F_o|$. ^b $R_2 = [\sum w(F_o^2 - F_c^2)^2 / \sum w(F_o^2)^2]^{1/2}$, $w = 1/[\sigma^2(F_o^2) + (aP)^2 + bP]$, $P = [\max(F_o^2, 0) + 2(F_c^2)]/3$, where $a = 0.0329$ and $b = 0.48$.

Table 2. Selected Bond Lengths (Å) and Angles (deg) for $\text{K}_5\text{Eu}_2\text{FSi}_4\text{O}_{13}$

Bond Lengths			
Eu(1)–O(1)	2.228(4) (2×)	Eu(1)–O(2)	2.269(5)
Eu(1)–O(4)	2.257(4) (2×)	Eu(1)–F(1)	2.550(4)
Eu(2)–O(6)	2.283(3) (2×)	Eu(2)–O(8)	2.284(3) (2×)
Eu(2)–O(9)	2.223(5)	Eu(2)–F(1)	2.490(4)
Si(1)–O(1)	1.600(4) (2×)	Si(1)–O(2)	1.629(5)
Si(1)–O(3)	1.665(5)	Si(2)–O(3)	1.628(5)
Si(2)–O(4)	1.581(4) (2×)	Si(2)–O(5)	1.642(5)
Si(3)–O(5)	1.645(5)	Si(3)–O(6)	1.593(3) (2×)
Si(3)–O(7)	1.646(6)	Si(4)–O(7)	1.667(5)
Si(4)–O(8)	1.611(3) (2×)	Si(4)–O(9)	1.607(6)
Bond Angles			
Eu(1)–F(1)–Eu(2)	177.5(2)	Si(1)–O(3)–Si(2)	137.6(4)
Si(2)–O(5)–Si(3)	132.4(3)	Si(3)–O(7)–Si(4)	135.9(3)

We report that $\Delta\rho_{\text{max,min}} = +1.95, -1.59 \text{ e } \text{\AA}^{-3}$. The residual electron densities in the final difference maps were close to those of Eu and K atoms. All calculations were performed using the SHELXTL version 5.1 software package.³³

Photoluminescence Measurements. Several crystals of **1** were contained in a glass capillary for luminescence study. A laser beam at 532 nm, which corresponds to the Eu^{3+} excitation to the $^3\text{D}_1$ state, from a diode laser, was employed as the light source to light up the powder sample for recording the emission spectra. The emission was collected by an $f/1$ focal lens and imaged onto a monochromator (Acton Research Corp. SP2300i) attached with a charge-coupled device (CCD, Andor DV 401A-BV) detector. To reduce the interference of laser light scattering, a 532 nm Notch filter was inserted in front of the monochromator. The typical emission spectrum was recorded at 15 mW and 10 min data acquisition time. This setup was also used for the measurements of emission radiative lifetime except the detector and the light source were replaced by a photomultiplier tube (PMT, Hamamatsu R636-10) and a tunable pulsed Nd:YAG laser (Spectra Physics INDI-40-10) and a pumped dye laser (Lambda Physik Scanmate 2E) beam, respectively.

Results and Discussion

Structure. The crystallographic data are given in Table 1, and selected bond lengths and bond angles are given in Table 2. The structure of **1** is constructed from the following building units: an unbranched tetrasilicate chain, $[\text{Si}_4\text{O}_{13}]$;

(32) Brown, I. D.; Altermatt, D. *Acta Crystallogr.* **1985**, *B41*, 244.

(33) Sheldrick, G. M. *SHELXTL Programs*, version 5.1; Bruker AXS GmbH: Karlsruhe, Germany, 1998.

a dimer of vertex-sharing octahedra, $[\text{Eu}_2\text{O}_{10}\text{F}]$; and five K sites. All K, Eu, Si, and F atoms lie in mirror planes. All O atoms in this oligosilicate anion are either bridging atoms O_{br} linking two Si atoms or terminal atoms O_{term} that coordinate to Eu atoms. All O_{br} atoms and two O_{term} atoms, O(2) and O(9), lie in mirror planes, and the other O atoms are at general positions. The Si–O distances range from 1.581 to 1.629 Å for O_{term} and from 1.628 to 1.667 Å for O_{br} . These values are within the normal ranges. The Si– O_{br} –Si bond angles are 137.6°, 132.4°, and 135.9° for O(3), O(5), and O(7), respectively, which are smaller than the mean value of 140° for the Si– O_{br} –O angles in 17 structures reported by Liebau.³⁴ The octahedral dimer consists of two octahedra with a fluorine atom as a common vertex. The bond angle at the bridging F atom is 177.5°. The Eu–F bonds are considerably longer than the Eu–O bonds. On the basis of the maximum cation–anion distance given by Donnay and Allmann,³⁵ a limit of 3.35 Å is set for K–O interactions, which gives the following coordination numbers: K(1), 10-coordinate, including two F atoms at 2.903 Å; K(2), 8-coordinate, including one F atom at 2.652 Å; K(3), 9-coordinate, including one F atom at 2.653 Å; K(4), 9-coordinate; K(5), 8-coordinate. The atomic displacement factors for all the K atoms are regular and normal, indicating that they are not loosely bound in the structure.

Compound **1** adopts a new structure. The connectivity between an octahedral dimer and a tetrasilicate chain is shown in Figure 1. Each octahedral dimer connects to 10 SiO_4 tetrahedra, which belong to 6 different tetrasilicate chains. Each chain connects to six dimers. In this way, a 3-D framework with 5- and 6-ring channels along the *b* axis is formed. K(1) is located in a cage surrounded by two octahedral dimers and six tetrahedra; K(2) is in a cage surrounded by two octahedral dimers and two six-membered rings formed by two octahedra and four tetrahedra; K(3) is in a cage similar to that for K(2); K(4) is in a cage surrounded by three six-membered rings formed by two octahedra and four tetrahedra and three four-membered rings formed by two octahedra and two tetrahedra; K(5) is in a cage similar to that for K(4).

Although a large number of lanthanide silicates are known, only a few lanthanide fluoride–silicates have been reported. For Eu, there are only two compounds, namely, $\text{KEu}^{\text{II}}_2\text{FSi}_4\text{O}_{10}$ and $\text{Eu}^{\text{II}}_2\text{Eu}^{\text{III}}_3\text{F}(\text{SiO}_4)_3$.^{36,37} They were prepared at high temperature by using KF or NaF as a flux under reducing conditions. The former contains strongly folded silicate sheets of connected four-membered rings, separated by interlayers of Eu^{2+} and F^- . The latter is a mixed-valence europium fluoride–silicate with an apatite-type structure. The structure contains isolated SiO_4^{4-} tetrahedra and two europium cation sites with coordination numbers of nine and seven, which are occupied by Eu^{2+} and Eu^{3+} cations, respectively. To our knowledge, compound **1** represents the first known europium(III) fluoride–silicate. Several fluoride–

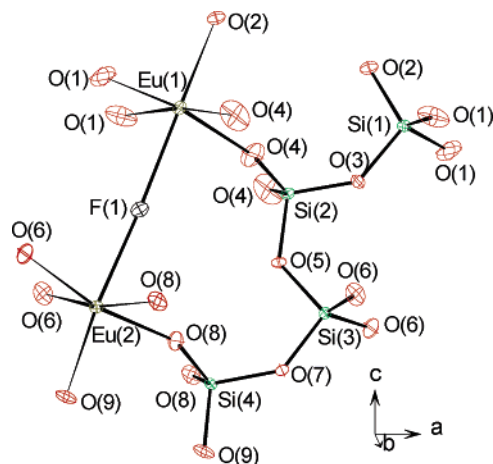


Figure 1. Connectivity between an octahedral dimer and a tetrasilicate chain, showing the atom labeling scheme. Thermal ellipsoids are shown at 50% probability.

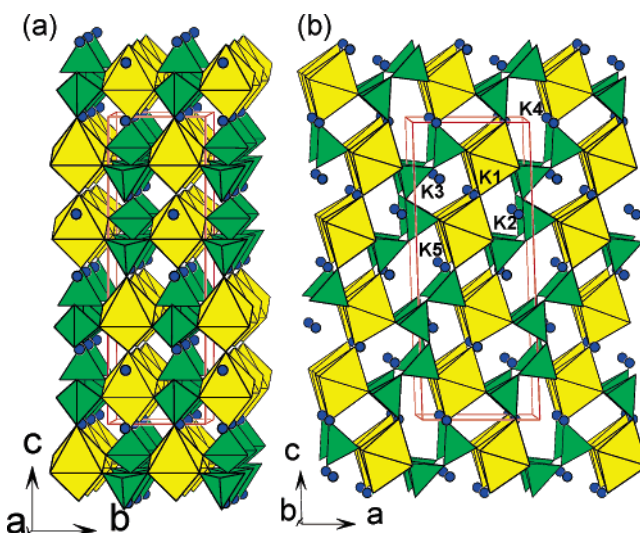


Figure 2. (a) Structure of **1** viewed along the *a* axis. The yellow and green polyhedra represent EuO_3F octahedra and SiO_4 tetrahedra, respectively. Blue circles are K atoms. (b) Structure of **1** viewed along the *b* axis.

silicates of Sc, La, Gd, Er, and Lu have also been reported, but all of them are different from **1** in both composition and crystal structure.

Photoluminescence Studies. Figure 3 shows the room-temperature (RT) emission spectrum of **1**. The RT excitation spectrum of **1** from 350 to 550 nm is depicted in the inset of Figure 3. The excitation lines are assigned to the Eu^{3+} intra- $4f^6$ transitions including the ${}^5\text{D}_{1-4} \leftarrow {}^7\text{F}_0$, ${}^5\text{L}_6 \leftarrow {}^7\text{F}_0$, and ${}^5\text{G}_1 \leftarrow {}^7\text{F}_0$ transitions. The RT emission spectrum recorded at 532 nm (${}^5\text{D}_1 \leftarrow {}^7\text{F}_0$) excitation exhibits a number of lines between 575 and 720 nm. These lines are ascribed to emission from the first excited ${}^5\text{D}_0$ state to the ${}^7\text{F}_{0-4}$ Stark levels of the fundamental Eu^{3+} septet. The emission lines originating from the higher electronic states such as ${}^5\text{D}_2$ and ${}^5\text{D}_1$ were not observed due to very efficient nonradiative relaxations, and this is evidenced by the fact that the emission spectrum at 473 nm excitation (${}^5\text{D}_2 \leftarrow {}^7\text{F}_0$) is identical to that shown in Figure 3. In the RT emission spectrum, two sharp lines corresponding to the ${}^5\text{D}_0 \rightarrow {}^7\text{F}_0$ transition were discerned. The presence of two ${}^5\text{D}_0 \rightarrow {}^7\text{F}_0$ lines clearly

(34) Liebau, F. *Structural Chemistry of Silicates: Structure, Bonding and Classification*; Springer-Verlag: Berlin, 1985.

(35) Donnay, G.; Allmann, R. *Am. Mineral.* **1970**, *55*, 1003.

(36) Jacobsen, H.; Meyer, G. Z. *Kristallogr.* **1994**, *209*, 348.

(37) Wickleder, C.; Hartenbach, I.; Lauxmann, P.; Schleid, T. *Z. Anorg. Allg. Chem.* **2002**, *628*, 1602.

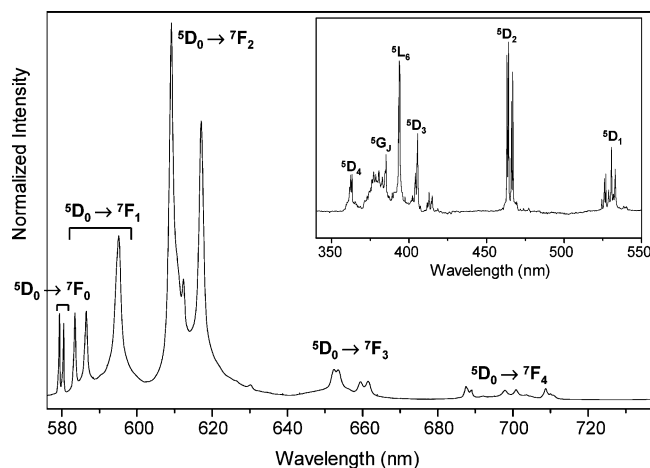


Figure 3. RT emission spectrum of **1** excited at 532 nm. The inset shows the excitation spectrum detected within the 7F_1 manifold (594 nm).

indicates the existence of at least two Eu^{3+} local environments, and this is consistent with the crystallographic results. Whereas the ${}^5D_0 \rightarrow {}^7F_{0,3}$ transitions are allowed due to the ligand field effects, the ${}^5D_0 \rightarrow {}^7F_1$ transitions have magnetic dipole (MD) character. On the other hand, the ${}^5D_0 \rightarrow {}^7F_{2,4}$ transitions in the 605–625 and 685–710 nm regions have electric dipole (ED) character and are allowed due to the lack of a symmetry center in the Eu^{3+} site. In contrast to the nearly equal integrated intensity between the ${}^5D_0 \rightarrow {}^7F_1$ and ${}^5D_0 \rightarrow {}^7F_2$ transitions in $\text{Cs}_3\text{EuSi}_6\text{O}_{15}$,²² the integrated intensity of the ${}^5D_0 \rightarrow {}^7F_2$ (ED) transition is much larger than that of the ${}^5D_0 \rightarrow {}^7F_1$ (MD) transition in compound **1**. These results confirm the crystallographic data; unlike the quite regular EuO_6 octahedron in $\text{Cs}_3\text{EuSi}_6\text{O}_{15}$,²² the EuO_5F octahedra in compound **1** lack inversion symmetry since a corner of the octahedron is now replaced by the F atom and the Eu–F bond distance (2.49–2.55 Å) is significantly greater than the Eu–O bond distance (2.23–2.27 Å);³⁸ i.e., the EuO_5F octahedra in **1** are strongly distorted. In addition, the emission lifetime of every line in the RT emission spectrum was measured at 532 nm excitation (${}^5D_1 \leftarrow {}^7F_0$) and at 473 nm excitation (${}^5D_2 \leftarrow {}^7F_0$). All the emission lines in the RT emission spectrum show the same decay curve, which can be well fit by a single-exponential decay function, as shown in Figure 4. It should be noted that the two emission lines corresponding to ${}^5D_0 \rightarrow {}^7F_1$ have the same decay curve at 532 nm excitation or 473 nm excitation, and this indicates no difference in the 5D_0 state radiative lifetimes of two Eu^{3+} sites. The simple decay curves indicate two facts. First, the observed emission is a simple radiative process and no other nonradiative processes occur in the 5D_0 state. Second, these two Eu^{3+} local environments are quite similar and this observation is verified by the crystallographic data. Nevertheless, it is quite interesting that the emission in compound **1** shows a much shorter lifetime of 2.0 ± 0.1 ms in comparison to the value (5.45 ms)²² in $\text{Cs}_3\text{EuSi}_6\text{O}_{15}$. Since there is no quenching group such as the hydroxyl group in **1** and the emission decay curves show the same single-exponential decay function, the shorter emission lifetime

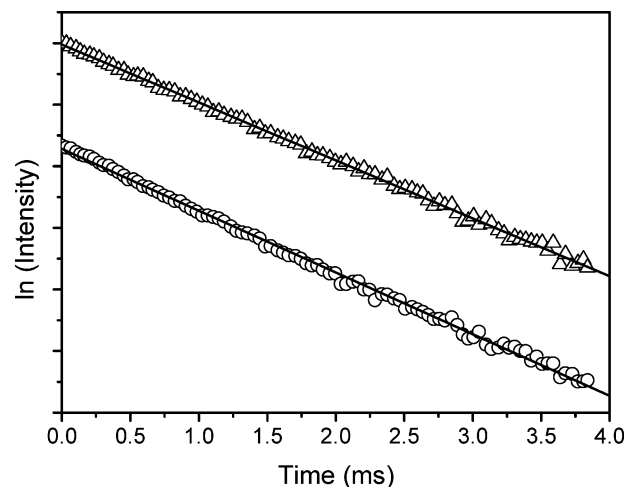


Figure 4. RT decay curves of the ${}^5D_0 \rightarrow {}^7F_1$ (○) and ${}^5D_0 \rightarrow {}^7F_2$ (△) transitions at 473 nm excitation. The intensity is in natural log scale, and the straight lines represent the best fit ($r^2 > 0.99$) to the data with a single-exponential decay function.

implies a larger electronic transition dipole moment in **1** than in $\text{Cs}_3\text{EuSi}_6\text{O}_{15}$. This phenomenon is supported by the observation that the emission intensities in **1** are brighter than those in $\text{Cs}_3\text{EuSi}_6\text{O}_{15}$.

In summary, the flux synthesis and crystal structure of a new europium fluoride–silicate have been reported. It is a new member of the open-framework lanthanide silicates, which contain stoichiometric amounts of framework lanthanide ions. Its structure consists of octahedral dimers of composition $[\text{Eu}_2\text{O}_{10}\text{F}]$ that are linked by unbranched tetrasilicate chains to form a 3-D framework. The luminescence properties have also been reported. The conclusions drawn from the number of peaks in the region for the ${}^5D_0 \rightarrow {}^7F_0$ transition and the relative intensities of the ${}^5D_0 \rightarrow {}^7F_1$ and ${}^5D_0 \rightarrow {}^7F_2$ transitions are in agreement with the crystallographic results. The lifetime measurement results indicate that the observed emission is a simple radiative process and no other nonradiative processes occur in the 5D_0 state, the coordination environments of two Eu^{3+} sites are quite similar, and there is a lifetime value of 2.0 ms. The synthesis of lanthanide silicates using a fluoride flux is of interest because the synthetic method prevents the presence of hydroxyl groups and water molecules, which are often detrimental to photoluminescence. Fine-tuning of luminescence properties may be achieved by introducing a second type of lanthanide ion in the framework. Further research to synthesize new lanthanide silicates and mixed-metal silicates by flux-growth and high-temperature/high-pressure hydrothermal methods is in progress.

Acknowledgment. We thank the National Science Council for support and Mr. Y.-S. Wen at the Institute of Chemistry, Academia Sinica, for the X-ray data collection.

Supporting Information Available: Crystallographic data for **1** in CIF format, a complete list of bond lengths and bond-valence sums, and X-ray powder patterns. This material is available free of charge via the Internet at <http://pubs.acs.org>.

(38) Carlos, L. D.; Videira, A. L. L. *Phys. Rev. B* **1994**, *49*, 11721.